New Weight Transform Schemes for Delayless Subband Adaptive Filtering

Jiaquan Huo, Sven Nordholm, Zhuquan Zang
Australian Telecommunications Research Institute,
Curtin University of Technology,
Wark Ave. Bentley, WA Australia
Phone: (618) 9266 3273

Abstract—**Very long adaptive filters are used for controlling the acoustic echo due to the acoustic echo of the loudspeaker and microphone. Subband adaptive filters have been proposed to save computations as well as speed up convergence. Delayless subband adaptive filters removes the additional signal path delay due to the analysis-synthesis system in their conventional counterpart by transforming the subband filters to a corresponding fullband one and cancelling the echo using the fullband filter. The weight transform from subband to fullband plays a crucial role in the delayless subband adaptive filters. In this paper, the defect of the FFT-stacking weight transform is identified, and new transform schemes are proposed. Simulation results show that significant performance improvements can be achieved by employing the proposed weight transform schemes.**

I. Introduction

In voice communication systems, acoustic echo arises when the loudspeaker signal is picked up by the microphone and transmitted back to the far-end speaker. The echo would be annoying if it returns a few milliseconds after the original speech, and in the extreme case it could completely disrupt a conversation [2]. Some kind of echo control is necessary in any communication system that produces round-trip delay larger than 32ms [1].

Traditional voice-activated switched-loss echo suppressors are half-duplex in nature and fail to perform satisfactory in systems with extremely long round trip delay. Echo cancellers have been introduced to provide full-duplex service. The basic idea of an echo canceller is to produce a synthesized echo from the far-end speech with an adaptive filter fine tuned to the echo path, and subtract this synthesized echo from the microphone signal. However, the acoustic echo path is typically of hundreds of milliseconds, and the adaptive filter used to identify the echo path would be of thousands of taps. Implementing such a long adaptive filter is computationally expensive. Moreover, such a long adaptive filter tends to converge slowly with speech signal as input. Subband adaptive filters have been proposed to save computation and improve convergence speed [5], [6], [7].

Conventional subband adaptive filters [6] cause undesirable additional signal path delay. Delayless subband adaptive filters [5], as illustrated in Fig. 1, eliminate the additional signal path delay. In a delayless subband adaptive filter, the echo path is identified in subbands with a set of parallel subband adaptive filters, and these subband filters are transformed to a corresponding fullband one with a weight transform, the fullband filter is used to cancel the echo. The delayless subband adaptive filter can operate in either an open-loop configuration, where local error signals are used to adapt the subband filters, or a closed-loop configuration, where fullband error signal is utilized.

This paper focuses on the weight transform for delayless subband adaptive filtering. This defect of the original FFT-stacking transform will be identified and new transform schemes will be proposed.

II. FFT-stacking Weight Transform

The FFT-stacking procedure suggested in [5] for the weight transform is illustrated in Fig. 2. Assume the fullband adaptive filter is N tap long, the echo path is identified in M subbands and the subband adaptive filters are of L taps. An L point FFT is calculated based on the filter weights in each subband, the resulting DFT coefficients are properly stacked in a N element array, and then the fullband filter impulse response is obtained as the IFFT of the N element array. The rules for stacking are as follows

1. For $l \in [0, N/2)$

$$H(l) = H_{[lM/N]}((l)_{2N/M})$$

where $H(l)$ and $H_k(l)$ stands for the lth DFT coefficient of the fullband filter and the kth subband filter respectively, $[a]$ is rounding a toward the nearest integer, and $(a)_b$ denotes 'a modulus b';
2. For $l = N/2$

$$H(N/2) = 0$$

3. For $l \in (N/2, N)$

$$H(l) = H(N-l)^*$$

where the superscript * denotes complex conjugate.

It can be shown that this weight transform is equivalent to constructing the fullband filter impulse response by passing the subband filter coefficients through a synthesis filter bank [4]

$$H(z) = \sum_{k=0}^{M-1} F_k(z) H_k(z^D) \tag{1}$$

0-7803-7206-9/01/$17.00 © 2001 IEEE

with synthesis filters given by

$$
\begin{aligned}
&F_k(z) = \\
&\begin{cases}
\sum_{l=-\frac{N}{2M}+1}^{\frac{N}{2M}-1} f(zW^l) & k=0 \\
\sum_{l=\frac{N}{2}-\frac{N}{2M},\, l\neq\frac{N}{2}}^{\frac{N}{2}+\frac{N}{2M}} f(zW^l) & k=\frac{M}{2} \\
\sum_{l=(2k-1)\frac{N}{2M}}^{(2k+1)\frac{N}{2M}-1} f(zW^l) & 0<k<\frac{M}{2} \\
\sum_{l=(2k-1)\frac{N}{2M}+1}^{(2k+1)\frac{N}{2M}} f(zW^l) & \frac{M}{2}<k<M-1
\end{cases} \\
&f(z) = \frac{1}{N}\sum_{l=-N+1}^{N-1} z^{-l} \\
&W = e^{-j\frac{2\pi}{N}}
\end{aligned} \tag{2}
$$

An example is given in Fig. 3. It can be seen that the synthesis filters have deep nulls in their passbands. This causes significant degradation in system performance.

III. Proposed Schemes

The synthesis filters for weight transform should ideally be be a set of ideal bandpass filters given by

$$
F_k(\omega) = \begin{cases} 1 & |\omega - \frac{2k\pi}{M}| < \frac{\pi}{M} \\ 0 & |\omega - \frac{2k\pi}{M}| > \frac{\pi}{M} \end{cases} \tag{3}
$$

Apparently this can only be approximated in practice.

A. FFT-2 Weight Transform

As can be seen in EQ. 2, the FFT-stacking weight transform sets the fullband filter response to zero at frequencies $\frac{(2l+1)\pi}{N}$, which results in the nulls within the passband of the synthesis filters. This can of cause be corrected by setting $H(\frac{(2l+1)\pi}{N})$ according to the frequency response of the proper subband filter. Therefore, the following weight transform, referred to as FFT-2, is proposed

$$
\begin{aligned}
&F_k(z) = \\
&\begin{cases}
\sum_{l=-\frac{N}{M}+1}^{\frac{N}{M}-1} f(zW^l) & k=0 \\
\sum_{l=N-\frac{N}{M},\, l\neq N}^{N+\frac{N}{M}} f(zW^l) & k=\frac{M}{2} \\
\sum_{l=(2k-1)\frac{N}{M}}^{(2k+1)\frac{N}{M}-1} f(zW^l) & 0<k<\frac{M}{2} \\
\sum_{l=(2k-1)\frac{N}{M}+1}^{(2k+1)\frac{N}{M}} f(zW^l) & \frac{M}{2}<k<M-1
\end{cases} \\
&f(z) = \frac{1}{2N}\sum_{l=-N+1}^{N-1} z^{-l} \\
&W = e^{-j\frac{2\pi}{2N}}
\end{aligned} \tag{4}
$$

This weight transform scheme can be implemented using fast convolution, as illustrated in Fig. 4. A $2L$, instead of L point FFT is calculated based on the L tap filter in each subband. The DFT coefficients of the subband filters are then stacked according to the following rules to form those of the fullband filter

1. For $l \in [0, N)$

$$H(l) = H_{[lM/2N]}((l)_{4N/M})$$

2. For $l = N$

$$H(N) = 0$$

3. For $l \in (N, 2N)$

$$H(l) = H(2N-l)^*$$

Finally, the fullband filter impulse response is the first N samples of the $2N$ point IFFT of $\{H(l)\}$.

The computation required for FFT-2 weight transform is as follows. The $2L$ point FFT for each subband requires $L\log_2 2L$ complex multiplications. Because the echo path is assumed to be real, only $M/2+1$ subband is required to be identified. Thus $(M/2+1)L\log_2 2L$ complex multiplications is required to obtain the DFT coefficients of the fullband filter. After that, $N\log_2 2N$ complex multiplications is required for the IFFT. Totally, the computational complexity of the FFT-2 weight transform counted in complex multiplications is $(M/2+1)L\log_2 2L + N\log_2 2N$.

B. DFT-FIR Weight Transform

Surely the ideal weight transform in EQ. 3 can also be expressed as a uniform DFT modulated filter bank

$$
\begin{aligned}
F_0(\omega) &= \begin{cases} 1 & |\omega| < \pi/M \\ 0 & |\omega| > \pi/M \end{cases} \\
F_k(z) &= F_0(zW^k) \\
W &= e^{-j\frac{2\pi}{M}}
\end{aligned} \tag{5}
$$

A Q tap linear phase FIR filter can be used to approximate the ideal lowpass prototype filter $F_0(\omega)$. By doing so, an initial extra delay of $(Q-1)/2$ samples is added to the fullband filter impulse response. This extra delay can be removed by starting the convolution at sample $(Q-1)/2$.

The DFT-FIR weight transform can implemented using a polyphase-FFT structure. Assuming critical decimation, with the polyphase representation [8], EQ. 1 can be written in matrix form as

$$\mathbf{H}(z) = \mathbf{E}(z)\mathbf{H}_{sb}(z) \tag{6}$$

where $\mathbf{H(z)}$ is an $M \times 1$ vector with its lth element being the lth polyphase component of the fullband filter, $\mathbf{E(z)}$ is an $M \times M$ matrix with its (l,k)th element as the lth polyphase component of the kth synthesis filter, and $\mathbf{H_{sb}(z)}$ is an $M \times 1$ vector whose kth element is the kth subband filter. Using the modulation structure of the synthesis filters, it becomes

$$\mathbf{H}(z) = \Lambda(z)\mathbf{W}^*\mathbf{H}_{sb}(z) \tag{7}$$

where $\Lambda(z)$ is a diagonal matrix with its lth diagonal element as the lth polyphase component of the prototype filter, and $\mathbf{W}$ is an $M \times M$ DFT matrix. For 2-times over-sampling systems, let $\mathbf{H}_{sb}(z) = \mathbf{H}^0_{sb}(z^2) + z^{-1}\mathbf{H}^1_{sb}(z^2)$, and

$$\mathbf{H}^i(z) = \Lambda(z)\mathbf{W}^*\mathbf{H}^i_{sb}(z) \tag{8}$$

the fullband filter $H(z)$ then can be expressed as

$$H(z) = H^0(z) + z^{-M/2}H^1(z) \tag{9}$$

where $H^i(z)$ is a sequence corresponding to $\mathbf{H^i(z)}$. Thus the polyphase-FFT network in Fig. 5 can be used for the DFT-FIR weight transform.

The DFT-FIR weight transform, implemented with polyphase-FFT network, requires L M point IFFT for computing $\mathbf{W}^*\mathbf{H}_{sb}(z)$, which is $\frac{LM}{2}\log_2 M$ complex multiplications, and LQ real multiplications for convolving the result from FFT with $\Lambda(z)$. This totals at about $2ML\log_2 M + LQ$ real multiplications.

IV. Simulation Results

Computer experiments are carried out to evaluate the performance of the echo cancellers employing the proposed schemes. The settings of the experiments are as follows:

- Echo path: The echo path is a 512 tap FIR filter as depicted in Fig. 6, estimated with data recorded in a car cabin;
- Far end signal: Far-end signal are taken as zero mean white noise with unit variance, color noise obtained by filtering a white noise with a first order IIR filter with a pole at 0.9 and a recorded female speech;
- Full band filter length: 512 taps;
- Adaptation parameters: Adaptation is carried out in 128 subbands with a decimation factor of 64. In the open-loop configuration, the subband filters are adapted by inverse QR decomposition based recursive least squares [3] algorithm with forgetting factor of 0.995, while in the closed-loop configuration, normalized LMS (NLMS) algorithm with stepsize 0.5 is used;
- Analysis filter bank is a uniform DFT-modulated filter bank with a 256 tap linear phase prototype filter designed as $fir1(255, 1/128)$;
- Prototype filter for DFT-FIR weight transform is a 383 tap linear phase filter designed as $fir1(382, 1/128)$.

Misalignment, defined as

$$\epsilon(n) = 20\log_{10}\left(\frac{\|\mathbf{h}_{opt} - \mathbf{h}(n)\|_2}{\|\mathbf{h}_{opt}\|_2}\right) \tag{10}$$

is plotted as the performance measurement.

Simulation results with open-loop configuration are plotted in Fig. 7 to 9. It is observed that the echo canceller employing the proposed schemes outperform that using FFT-stacking by about 10 to 15 dB. In Fig. 10 and 11, it is shown that the misalignment goes as low as to -280 dB, where machine precision is -300 dB, which means almost ‘alias free’ performance can be obtained with a closed-loop delayless adaptive filter equipped with the proposed schemes. This desired feature is not observed in Fig. 12 due to the fact that the excitation at the highest frequencies is very poor, only at the level of 10^{-10}. Moreover, the slow convergence associated with the closed-loop structure is not witness when the proposed schemes are employed.

V. Conclusion

In this paper, the weight transform from subband to fullband for delayless subband adaptive filters is interpreted as a synthesis filter bank and the defect of the FFT-stacking is identified as the nulls in the passbands of the synthesis filters. Two new weight transform schemes, namely the FFT-2 and the DFT-FIR, are proposed, and their implementation discussed. Simulation results show that significant improvements in performance, in terms of steady state error level and convergence speed, can be achieved by employing the proposed schemes.

References

[1] International Engineering Consortium, *Echo cancellation tutorial*, http://www.webproforum.com/echo_cancel/topic07.htm, 2000.

[2] S.L. Gay, *An introduction to acoustic echo and noise control*, Acoustic Signal Processing for Telecommuniication (Steven L. Gan and Jacob Benesty, eds.), Kluwer Academic Publishers, 2000.

[3] S. Haykin, *Adaptive filter theory*, 3rd ed., Prentice-Hall, Upper Saddle River, NJ 07458, 1996.

[4] J. Huo, S. Nordholm, and Z. Zang, *A new subband to fullband transformation for delayless subband adaptive filtering*, IFCC’00 (Bankok), 2000.

[5] D.R. Morgan and J.C. Thi, *A delayless subband adaptive filter architecture*, IEEE Transactions on Signal Processing **43** (1995), no. 8, 1819–1830.

[6] J.J. Shynk, *Frequency-domain and multirate adaptive filtering*, IEEE Signal Processing Magzine (1992), 14–37.

[7] M.M. Sondhi and W. Kellermann, *Adaptive echo cancellation for speech signals*, Advances in Speech Signal Processing (Sadavki Furui and M. Mohan Sondhi, eds.), Marcel Dekker Inc., 1992.

[8] P.P. Vaidyanathan, *Multirate systems and filter banks*, Prentice Hall, 1993.

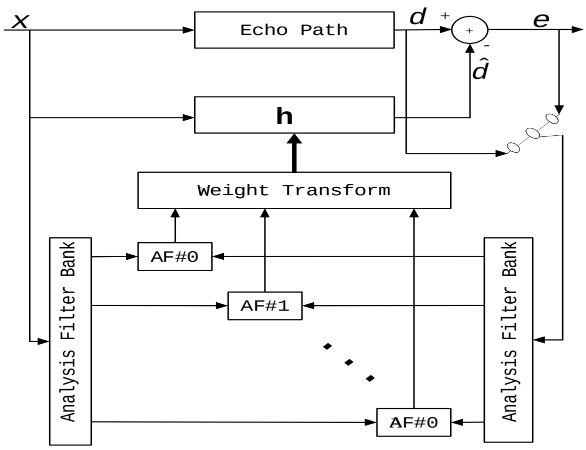

Fig. 1. Basic configuration of delayless subband adaptive Filters

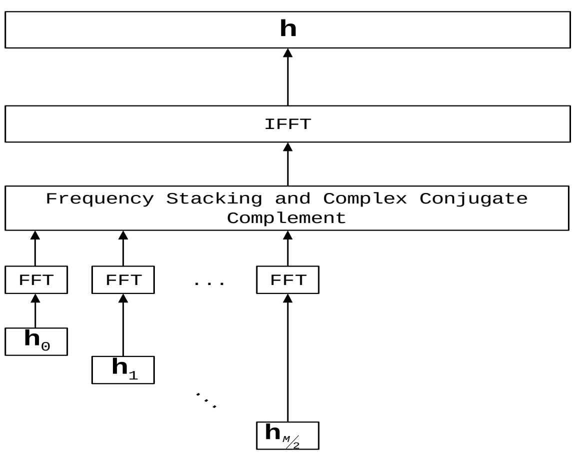

Fig. 2. FFT-Stacking weight transform

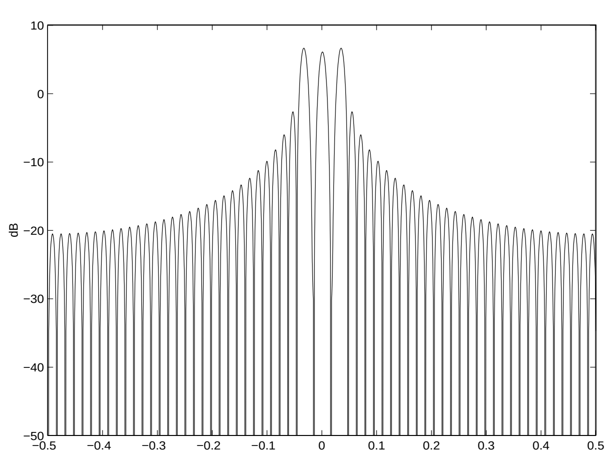

Fig. 3. Frequency response of the 0th synthesis filter for FFT-stacking weight transform, $N = 32$, $M = 8$

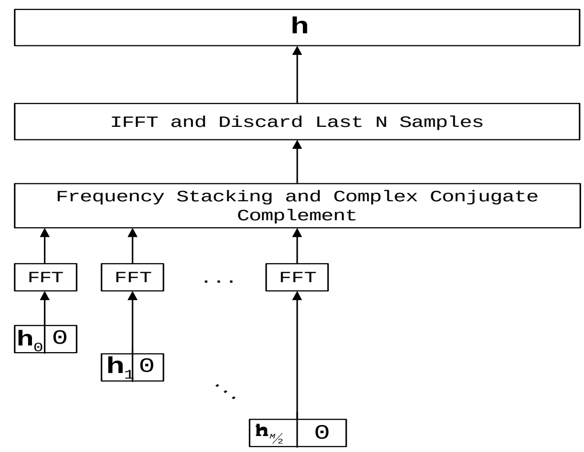

Fig. 4. FFT-2 weight transform

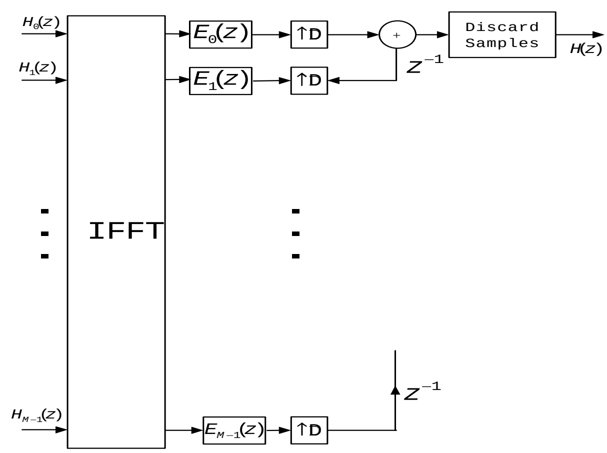

Fig. 5. DFT-FIR weight transform

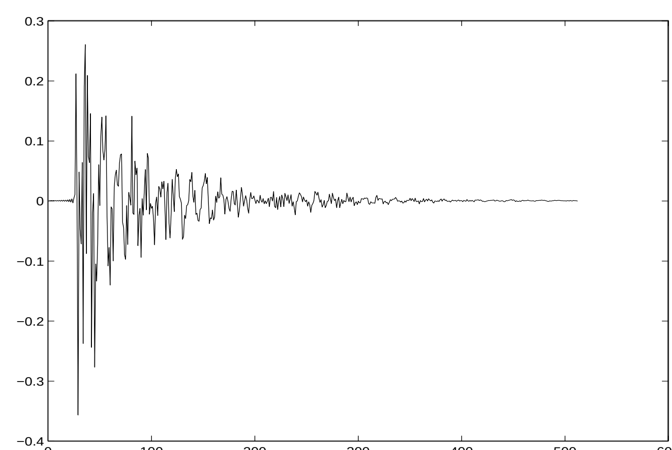

Fig. 6. Echo path used in simulation

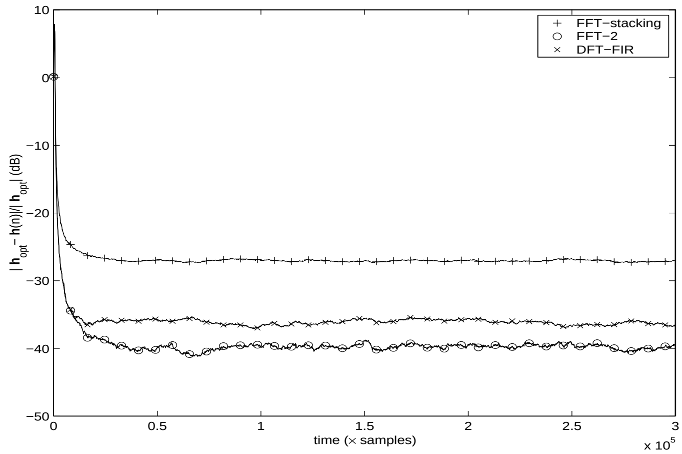

Fig. 7. Performance comparison of different weight transform schemes: open-loop with white noise input

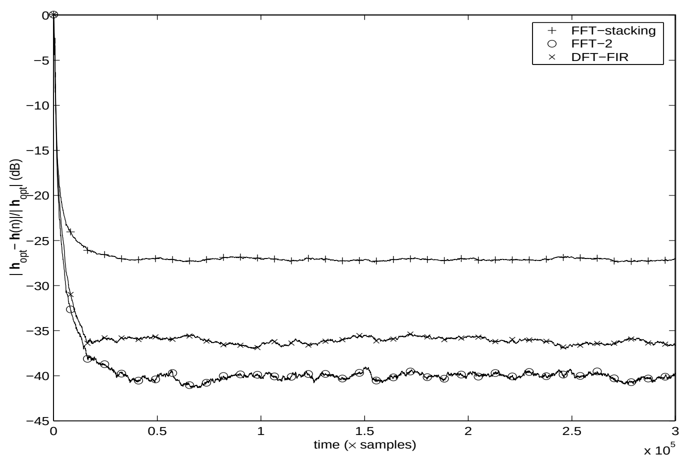

Fig. 8. Performance comparison of different weight transform schemes: open-loop with color noise input

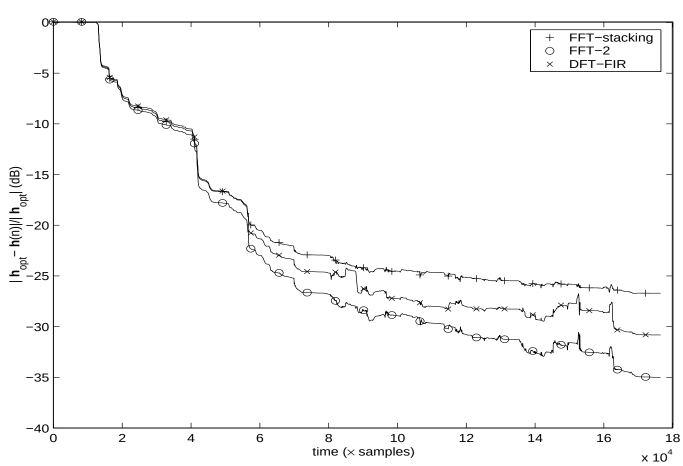

Fig. 9. Performance comparison of different weight transform schemes: open-loop with speech input

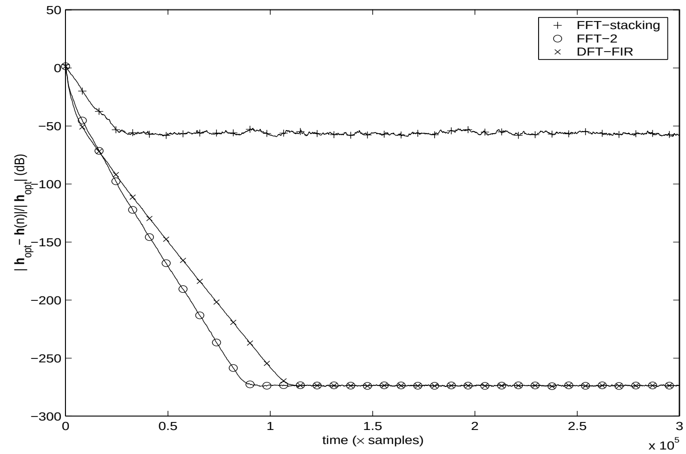

Fig. 10. Performance comparison of different weight transform schemes: closed-loop with white noise input

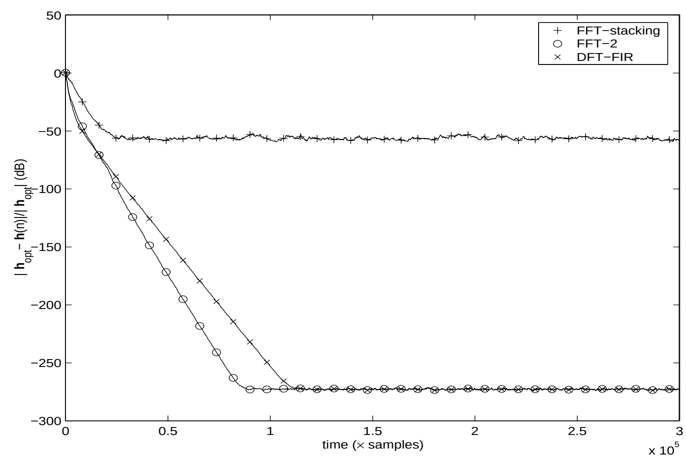

Fig. 11. Performance comparison of different weight transform schemes: closed-loop with color noise input

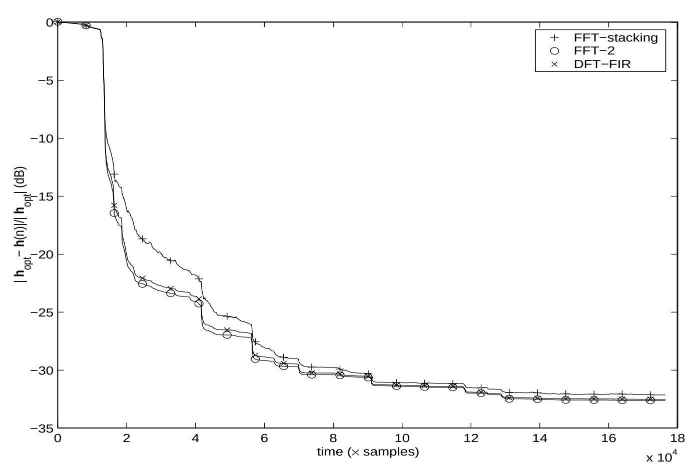

Fig. 12. Performance comparison of different weight transform schemes: closed-loop with speech input